Simulation of Atmospheric Air Micro Plasma Jet for Biomedical Applications

Luke T. Gritter[1], Jeffrey S. Crompton[*1], and Kyle C. Koppenhoefer[1]
[1]AltaSim Technologies, LLC 130 E. Wilson Bridge Rd, Suite 140, Columbus, OH
*Corresponding author: jeff@altasimtechnologies.com

Abstract: Small-scale plasma jets in atmospheric air can produce regions of highly reactive chemistry that are near room temperature. This type of cold plasma jet is useful for decontamination of surfaces and sterilization of living tissue, and simulation can be used to help design a plasma jet that maximizes the extent and effectiveness of surface treatment while maintaining a sufficiently low temperature to avoid damaging sensitive surfaces. In the device under consideration in this work, atmospheric pressure air is forced through a hollow anode and cathode. Immediately prior to exiting the device, the air is subjected to a strong electric field, resulting in a plasma jet. The small diameter of the plasma and the turbulent heat transfer in the flow facilitate a low jet temperature, while reactive species continue to exist for some distance away from the nozzle. Due to the strong coupling between the electric field, fluid flow, physical kinetics, chemical reactions, and heat transfer, the simulation of plasma jets is a challenging multiphysics problem. A fully coupled plasma, fluid flow, and heat transfer analysis of the plasma jet has been conducted using COMSOL Multiphysics®, and the simulation results used to predict the temperature distribution and the concentrations of reactive species within the jet.

Keywords: Plasma jet, chemical reactions, turbulent flow, heat transfer.

1. Introduction

The highly reactive chemistries of air plasmas make them attractive for use in surface cleaning and sterilization, but there are two difficulties associated with using this type of plasma in these applications. First, the excitation of air plasmas at atmospheric pressure typically results in temperatures that are too high for use on sensitive materials or living tissues. Second, plasmas in atmospheric pressure air tend to exhibit filamentation and arcing, resulting in an unstable plasma and causing damage to adjacent surfaces.

These difficulties can be overcome by utilizing a microscale plasma torch. In this device, the small size scale enables the excitation of a stable DC discharge at atmospheric pressure, while the small diameter of the plasma jet and the turbulence generated in the shear layer facilitate rapid cooling of the plasma as it flows into the ambient air. This process can produce a continuous flow of air with a reactive chemistry and a temperature that is not far above ambient. An array of these micro plasma jets could be used to facilitate a larger coverage area.

The device under consideration in this work is illustrated in Figure 1. A hollow anode is situated inside a hollow cathode, and these electrodes are separated by an insulator with a thickness of 0.2 mm. Air flow in the hollow anode is forced through a 0.2 mm diameter throat within which the plasma is excited, and the plasma jet exits the torch through a hole in the grounded cathode into the ambient air.

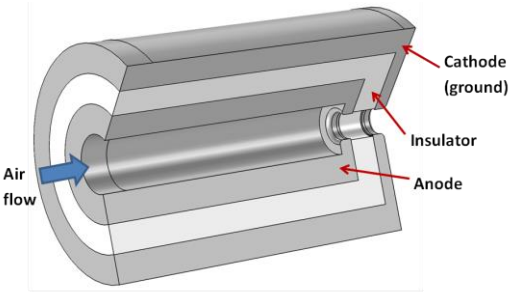

Figure 1. Cutaway of microscale plasma torch geometry.

In the design of a microscale plasma torch for surface cleaning and sterilization applications, it is desirable to maximize the coverage area and the reactive species concentrations and to minimize the temperature of the jet. The key design parameters that influence these characteristics include the air flow rate, the throat diameter, the insulation thickness, and the

electric potential at the anode. The model developed in this work can be used to evaluate the effects of design and operating parameters and thus allow optimization of the plasma torch.

2. Model Description

Plasma jets are inherently multiphysics phenomena, featuring a coupled system of electromagnetics, physical kinetics, chemical reactions, turbulent flow, and heat transfer. The strong coupling between the various physics and the non-linearity of the system result in a challenging numerical problem. Simulation of atmospheric pressure air plasmas can be particularly difficult due to numerical instability at high pressures and the large number of species and reactions. To simulate this challenging physical system, an axisymmetric model including the plasma physics, turbulent flow, and heat transfer has been constructed and solved using COMSOL Multiphysics®.

A non-equilibrium model is necessary to obtain the species concentrations along the jet, and the high pressure flowing plasma can be suitably approximated using a fluid approach. For the electrons, this is accomplished by means of drift-diffusion equations for the transport of the electron density and the electron energy density:

$$\frac{\partial n_e}{\partial t} + \nabla \cdot \left(\mu_e n_e \nabla V - D_e \nabla n_e\right) + \mathbf{u} \cdot \nabla n_e = R_e \qquad (1)$$

$$\begin{aligned} &\frac{\partial n_\varepsilon}{\partial t} + \nabla \cdot \left(\mu_\varepsilon n_\varepsilon \nabla V - D_\varepsilon \nabla n_\varepsilon\right) \\ &-\nabla V \cdot \left(\mu_e n_e \nabla V - D_e \nabla n_e\right) + \mathbf{u} \cdot \nabla n_\varepsilon = S_{en} \end{aligned} \qquad (2)$$

In the above equations, n_e is the electron density, n_ε is the electron energy density, V is the electric potential, $\mathbf{u}$ is the velocity vector of the bulk gas, μ_e and μ_ε are mobilities, D_e and D_ε are diffusivities, R_e is an electron source term due to ionization and attachment reactions, and S_{en} is an energy source term due to collisions.

The mobilities, diffusivities, and electron impact reaction rates are required inputs to the drift-diffusion equations, but they are strongly dependent upon the electron energy distribution function (EEDF), which is not known beforehand. To provide these inputs, the Boltzmann Equation, Two-Term Approximation physics interface in the COMSOL Multiphysics Plasma Module was used to solve for a non-Maxwellian EEDF for an air plasma chemistry over a range of mean electron energies. From these results, interpolation tables were generated for the transport coefficients and the electron impact reaction rates as a function of mean electron energy, and these tables were used as inputs to the fluid model of the plasma.

The feed air is assumed to be composed of 80 percent nitrogen and 20 percent oxygen at atmospheric pressure, and the ignition of a plasma in such a mixture results in an extremely complex chemistry. In the present work, a somewhat simplified chemistry has been constructed that includes six ground state species, three metastables, seven positive ions, and three negative ions, as shown in Table 1.

Neutrals	N_2, $N_2(A^3\Sigma)$, $N_2(a'^1\Sigma)$, N, O_2, O_2(m)*, O, O_3, NO
Positive Ions	N^+, N_2^+, N_4^+, O^+, O_2^+, O_4^+, NO^+
Negative Ions	O^-, O_2^-, O_3^-

Table 1. Species included in plasma chemistry. * O_2(m) combines $O_2(a^1\Delta)$ and $O_2(b^1\Sigma)$ metastables.

The transport of each of these heavy species is described by an equation of the following form:

$$\rho \frac{\partial \omega_i}{\partial t} + \nabla \cdot \mathbf{j_i} + \rho(\mathbf{u} \cdot \nabla)\omega_i = R_i \qquad (3)$$

In this equation, ω_i is the mass fraction of species i, ρ is the gas density, R_i is a source term due to reactions, and $\mathbf{j_i}$ is the diffusive flux vector, which also includes the flux due to migration in the electric field if the species is an ion. The air plasma chemistry used in this work contains 183 reactions, including 63 electron impact reactions.

The variation in the electric potential is governed by Poisson's equation for electrostatics:

$$\nabla \cdot \left(-\varepsilon_0 \varepsilon_r \nabla V\right) = \rho_q \qquad (4)$$

The space charge ρ_q is the sum of the ion and electron charge densities, and the effect of this term on the electric field results in strong coupling between the ion transport and the electron transport. The anode is connected to a small circuit with a ballast resistor between the anode and the voltage source and a blocking capacitor between the anode and ground, as shown in Figure 2.

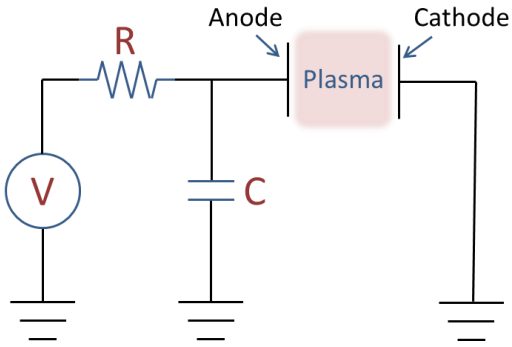

Figure 2. Diagram of circuit connected to anode.

The fluid is assumed to be an ideal gas, and the conservation of mass and momentum in the fluid are described by the continuity equation (Equation 5) and the Navier-Stokes equations (Equation 6), respectively:

$$\frac{\partial \rho}{\partial t} + \nabla \cdot (\rho \mathbf{u}) = 0 \quad (5)$$

$$\rho \frac{\partial \mathbf{u}}{\partial t} + (\mathbf{u} \cdot \nabla)\mathbf{u} = -\nabla p + \nabla \cdot \left[(\mu + \mu_T)\left(\nabla \mathbf{u} + (\nabla \mathbf{u})^T - \frac{2}{3}(\nabla \cdot \mathbf{u})\mathbf{I} \right) - \frac{2}{3}\rho k \mathbf{I} \right] \quad (6)$$

In the Navier-Stokes equations, μ is the dynamic viscosity, μ_T is the eddy viscosity, and k is the turbulent kinetic energy. The eddy viscosity and turbulent kinetic energy are calculated using the k-ε turbulence model.

Conservation of energy is maintained by solving an energy equation for the temperature. In the gas, this equation takes the following form:

$$\rho c_p \frac{\partial T}{\partial t} + \rho c_p \mathbf{u} \cdot \nabla T + \nabla \cdot \left[-(\lambda + \lambda_T)\nabla T \right] = Q \quad (7)$$

The variable T is the temperature, c_p is the specific heat capacity at constant pressure, λ is the thermal conductivity of the gas, λ_T is the turbulent thermal conductivity, and Q is a heat source term. The Kays-Crawford model is used to calculate the turbulent thermal conductivity as a function of the eddy viscosity and the local gas properties. The heat source accounts for both the energy imparted to the gas from the electrons by means of collisions with heavy species and the energy imparted to the gas by the acceleration of ions in the electric field, the effect of radiation has not been included. For the conditions explored in this work, the pressure work term is small and has been neglected.

3. Results

The operation of the micro plasma torch was simulated for a flow rate of 80 ml/min and an applied voltage of 1000 V with a 100 kΩ ballast resistor, and a stationary solution was obtained. Under steady-state operation, the anode voltage is 550 V, and the discharge current is 4.5 mA.

The temperature profile of the plume is shown in Figure 3, and Figure 4 gives the temperature on the jet axis. At a distance of 10 mm from the torch exit, the centerline jet temperature has dropped to 92 °C. A peak temperature of about 1900 °C occurs in the cathode sheath.

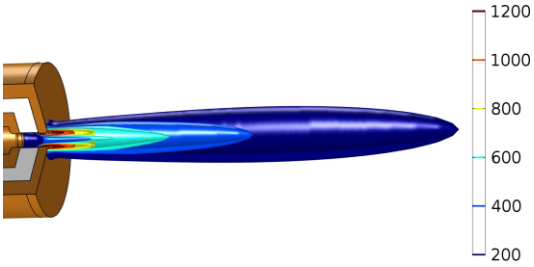

Figure 3. Isosurfaces of gas temperature (°C).

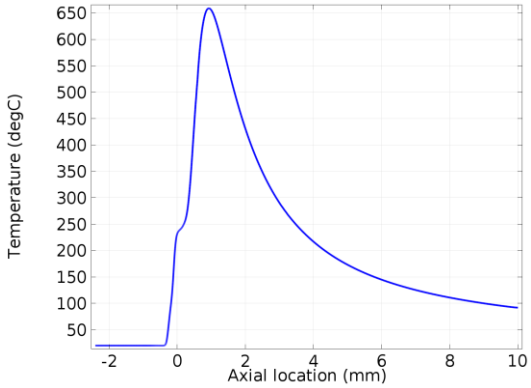

Figure 4. Temperature along jet axis (exit from torch is at 0 mm).

Figure 5 shows the velocity magnitude of the gas on a slice through the jet axis, and the velocity magnitude along the jet axis is given in Figure 6. After the jet exits the torch, the velocity quickly drops as the plume diameter increases and the gas cools. The jet has a peak Mach number of about 0.35 as it exits the torch.

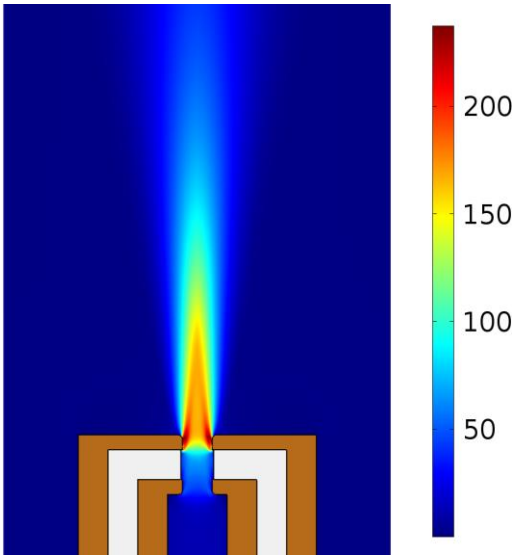

Figure 5. Velocity magnitude (m/s) on slice through jet axis.

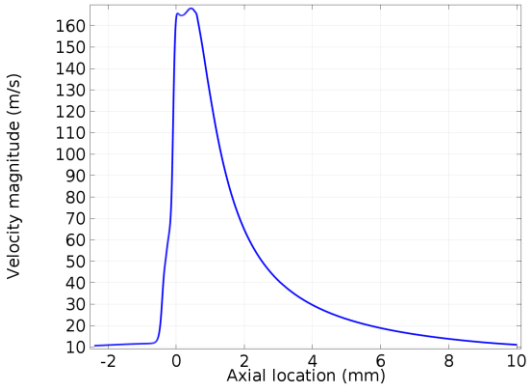

Figure 6. Velocity magnitude along jet axis (exit from torch is at 0 mm).

The simulation results indicate that significant concentrations of reactive species persist in the plume even after the gas temperature has dropped below 100 °C. Figures 7 and 8 plot the distribution of O_2^+ and O_3^- ions, respectively, and Figure 9 shows the number density of various ions along the jet axis. The distribution of atomic oxygen in shown in Figure 10, and the number densities of various neutral species on the jet centerline are given in Figure 11.

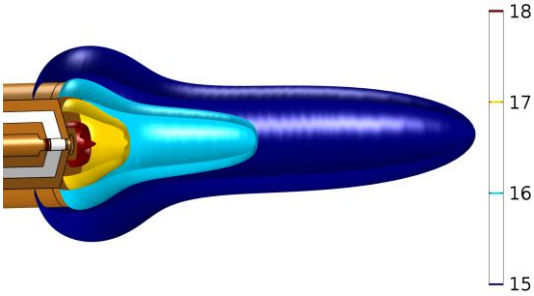

Figure 7. Isosurfaces of $\log_{10}$ of O_2^+ number density (m^{-3}).

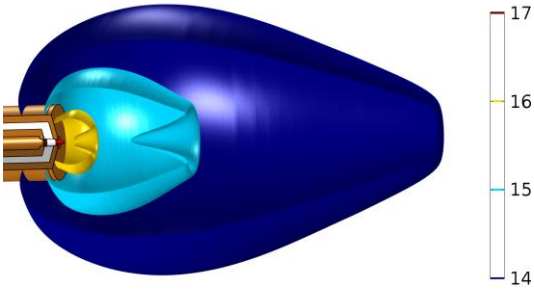

Figure 8. Isosurfaces of $\log_{10}$ of O_3^- number density (m^{-3}).

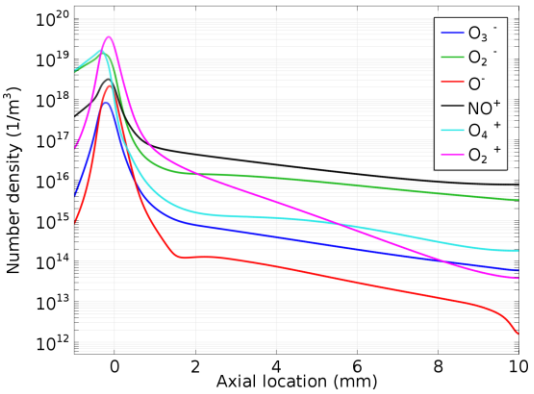

Figure 9. Ion number density along jet axis (exit from torch is at 0 mm).

At a distance of 10 mm from the torch exit, the electron density has dropped to about 4×10^{13} m^{-3}, but reactive heavy species remain at much higher number densities. The total ion density at this location is about 10^{16} m^{-3}, and the highly reactive atomic oxygen radical is present at a number density greater than 10^{15} m^{-3}. The simulation results also show production of high concentrations of ozone and nitric oxide, but the persistence of nitric oxide is overestimated by the model, as the formation of nitrogen dioxide was not included in the air plasma chemistry.

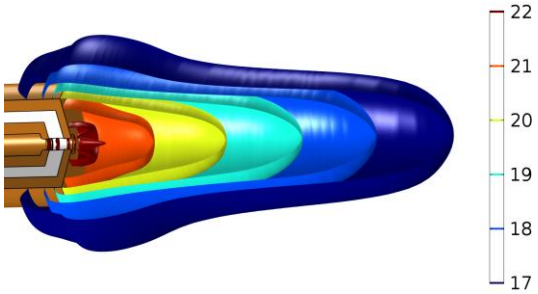

Figure 10. Isosurfaces of $\log_{10}$ of atomic oxygen number density (m^{-3}).

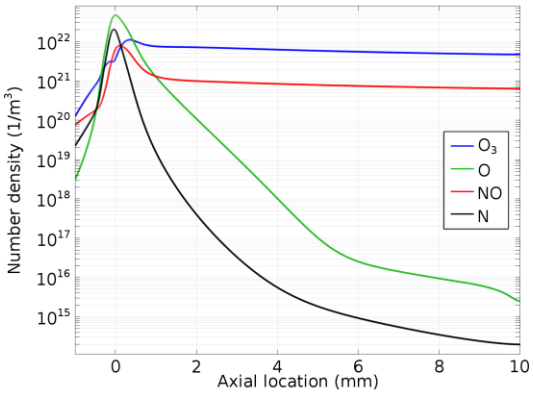

Figure 11. Neutral number density along jet axis (exit from torch is at 0 mm).

4. Summary

A model of a microscale plasma torch has been built and solved in COMSOL Multiphysics. The model includes the plasma, turbulent flow, and heat transfer physics that are necessary to simulate a micro plasma jet, and it can be used to predict temperature and species distributions throughout the plume. The simulation results show that a reactive chemistry persists in the jet even as the gas temperature approaches ambient, and the model can be used to optimize the design of micro plasma torches for cleaning and sterilization of living tissues or other sensitive materials.